



The magneto-Hall difference and the planar extraordinary Hall balance

S. L. Zhang and T. Hesjedal

Citation: *AIP Advances* **6**, 045019 (2016); doi: 10.1063/1.4948443

View online: <http://dx.doi.org/10.1063/1.4948443>

View Table of Contents: <http://scitation.aip.org/content/aip/journal/adva/6/4?ver=pdfcov>

Published by the *AIP Publishing*

Articles you may be interested in

Critical anomalous Hall behavior in Pt/Co/Pt trilayers grown on paper with perpendicular magnetic anisotropy
Appl. Phys. Lett. **104**, 262404 (2014); 10.1063/1.4885775

Monitoring magnetization reversal and perpendicular anisotropy by the extraordinary Hall effect and anisotropic magnetoresistance.

J. Appl. Phys. **108**, 043924 (2010); 10.1063/1.3475690

Thickness dependence of parallel and perpendicular anisotropic resistivity in Ta/NiFe/IrMn/Ta multilayer studied by anisotropic magnetoresistance and planar Hall effect

J. Appl. Phys. **101**, 053702 (2007); 10.1063/1.2435816

Hall effect and magnetic properties of III-V based (Ga_{1-x}Mn_x)As/AlAs magnetic semiconductor superlattices

J. Appl. Phys. **83**, 6551 (1998); 10.1063/1.367577

Magnetoresistance, Hall effect, and thermoelectric power in spin valves

J. Appl. Phys. **83**, 5927 (1998); 10.1063/1.367457



NEW Special Topic Sections

NOW ONLINE
Lithium Niobate Properties and Applications:
Reviews of Emerging Trends

AIP Applied Physics Reviews

The magneto-Hall difference and the planar extraordinary Hall balance

S. L. Zhang and T. Hesjedal^a

Clarendon Laboratory, Department of Physics, University of Oxford, Parks Road, Oxford, OX1 3PU, United Kingdom

(Received 25 February 2016; accepted 20 April 2016; published online 27 April 2016)

The extraordinary Hall balance (EHB) is a general device concept that harnesses the net extraordinary Hall effect (EHE) arising from two independent magnetic layers, which are electrically in parallel. Different EHB behavior can be achieved by tuning the strength and type of interlayer coupling, i.e., ferromagnetic or antiferromagnetic of varying strength, allowing for logic and memory applications. The physics of the EHE in such a multilayered systems, especially the interface-induced effect, will be discussed. A discrepancy between the magnetization and the Hall effect, called the magneto-Hall difference (MHD) is found, which is not expected in conventional EHE systems. By taking advantage of the MHD effect, and by optimizing the materials structure, magnetoresistance ratios in excess of 40,000% can be achieved at room-temperature. We present a new design, the planar EHB, which has the potential to achieve significantly larger magnetoresistance ratios. © 2016 Author(s). All article content, except where otherwise noted, is licensed under a Creative Commons Attribution (CC BY) license (<http://creativecommons.org/licenses/by/4.0/>). [<http://dx.doi.org/10.1063/1.4948443>]

I. INTRODUCTION

The pace of the improvement of computing hardware has been slowing down, also because the device technologies it is built on have been nearly optimized to their limits. Attempts to overcome these challenges will have to be cross-disciplinary and will have to come up with radically new ways to process, store, and communicate information. Nanomagnetic solutions are promising for memory and logic applications. Such so-called hysteretic materials and devices are characterized by a large, switchable resistance, energy efficiency, and non-volatility.¹

The success of magnetic random access memory (MRAM),² which builds on magnetic tunnel junctions (MTJs), and which has been proposed to be used for both memory and logic gates,³ has also been affected by the low magnetoresistance ratios (MRRs). MTJs are composed of an insulating spacer (MgO), serving as a tunneling barrier, separating two independent ferromagnetic (FM) layers. The tunneling MR (TMR) reflects the magnetization configuration of the two FM layers, and is defined as $TMR = (R_{\uparrow\downarrow} - R_{\uparrow\uparrow}) / R_{\uparrow\uparrow}$. If the two magnetizations are parallel ($\uparrow\uparrow$, $\downarrow\downarrow$), the resistance is low, and in the antiparallel case ($\uparrow\downarrow$, $\downarrow\uparrow$) it is high. The spin polarization in the two FM layers is $p_i = (N_{Mi} - N_{mi}) / (N_{Mi} + N_{mi})$, $i = 1, 2$. p_i is a parameter that describes how much the spin population is ‘split’ between the two states, where N_i is the density of states of the FM layer i , and N_{Mi} and N_{mi} denote the majority and minority spins. When electrons pass from layer 1 to layer 2, the dielectric layer provides an ultrahigh barrier to the conduction electrons, thus the conductance G is proportional to the tunneling probability $P(1 \rightarrow 2)$, a linear function of $N_{\uparrow 1}N_{\uparrow 2} + N_{\downarrow 1}N_{\downarrow 2}$. Therefore, there are two different G values based on the different magnetization configurations, and one can write $G_{\uparrow\uparrow} \sim N_{M1}N_{M2} + N_{m1}N_{m2}$, while $G_{\uparrow\downarrow} \sim N_{M1}N_{m2} + N_{m1}N_{M2}$. Together with the definition of the spin polarization, the definition for the TMR can be rewritten as $TMR = (2p_1p_2) / (1 - p_1p_2)$. MTJs have achieved much in the past decades as nonvolatile, high-density, long-lifetime, fast, and

^aThorsten.Hesjedal@physics.ox.ac.uk

low-power elements.⁴ For the use as a memory device, the MTJ's TMR is the most crucial parameter as it determines how easily a circuit can distinguish between the two states (assigning $\uparrow\uparrow$ as '1' and $\uparrow\downarrow$ as '0'). For a typical transistor, the ratio between states exceeds 10^5 . On the other hand, the largest reported room-temperature TMR value is below 1,000% (see, e.g. Ref. 5).

The reason for this low TMR value is rather obvious inspecting the TMR equation: the TMR is controlled by the spin polarizations in both FM layers. As a full spin polarization of 100% is experimentally not achievable (even half-metals have a less than unity spin polarization at finite temperatures), the TMR is intrinsically limited by its system design. Novel approaches to reach higher TMR values are based on novel materials, such as ultra-high spin polarization Heusler compounds, or novel physical effects, which have not been explored in this context, such as the metal-to-insulator transition or ferroelectric tunnel junctions.¹

From the above evaluation of the MTJ, it can be seen that novel designs are required to address its fundamentally limiting issues. An ideal solution is a new device element that inherits the advantages of an MTJ, while the readout scheme is radically altered, overcoming the limitation given by the expression for the TMR, and resulting in an unlimited MRR between the two physical states. Recently, we introduced a new device concept, the extraordinary Hall balance (EHB).⁶ This device concept is remarkably simple since it only uses conventional ferromagnets and amorphous or polycrystalline barriers, yet shows MRRs of more than 40,000% at room-temperature.⁷ The basic device element can be precisely tuned to allow for the embedding of added functionalities.^{7,8} Also, owing to its simplicity in terms of materials and processing, complex heterostructures can be grown which function as multi-valued memory stacks.⁹ In a sense, an EHB is a special type of MRAM, which consists of two ferromagnetic stacks separated by an insulating layer. The device is read out by measuring the Hall voltage across the structure. As the two ferromagnetic layers switch independently, the Hall voltages — which can be positive or negative — add up to be either large and positive or negative, or almost vanishing. Minimizing the compensated, low Hall voltage state is key in the quest to increasing the MRR by another 1-2 orders of magnitude (to reach an ON-OFF ratio of 10^4), and the focus of this paper. The main challenge lies in the discrepancy between the magnetic and electric effects, the so-called magneto-Hall difference (MHD), which is not found in single-layer extraordinary Hall effect systems. Here, we present a study of the MHD effect, and by using it to our advantage, a further increase of the MRR can be achieved. Finally, we introduce a new planar EHB design that overcomes these challenges by separating the functional elements spatially.

II. EXTRAORDINARY HALL EFFECT IN MULTILAYERS

The extraordinary Hall effect (EHE) – or anomalous Hall effect – occurs in ferromagnetic materials in which the magnetization M , instead of the external field H , is causing the Hall voltage V_{xy} . The *ordinary* Lorentz-force-induced Hall effect and the EHE are always occurring together when measuring the V_{xy} in magnetic systems. However, the ordinary Hall effect is smeared out for large carrier densities as they are typical for metallic, itinerant ferromagnets, and can therefore be neglected here.

The intrinsic part of the EHE can be essentially regarded as an asymmetric version of the spin Hall effect, which originates from the spin-orbit interaction.¹⁰ For uniformly magnetized ferromagnetic media, the spin-polarized band structure gives rise to a (magnetic) conductivity vector, when integrated over the Brillouin zone (BZ):¹¹

$$\vec{\sigma}^M = -\frac{e^2}{\hbar} \int_{\text{BZ}} \frac{d^3k}{(2\pi)^3} \vec{\Omega}_k, \quad (1)$$

where $\sigma_k^M = (1/2)\epsilon_{ijk}\sigma_{ij}^M$ with the antisymmetric tensor ϵ_{ijk} , and $\vec{\Omega}_k = \sum_n f_{n\vec{k}} \vec{\Omega}_{n\vec{k}}$, where $f_{n\vec{k}}$ is the Fermi-Dirac distribution and $\vec{\Omega}_{n\vec{k}}$ is the Berry phase curvature. The conductivity component in the measurement direction (usually σ_{xy}^M) gives the EHE resistivity $\rho_{xy}^M = \rho_{xx}^2 \sigma_{xy}^M$, where ρ_{xx} is the longitudinal resistivity for the current applied along the x -direction. For thin films, the relationship of the measured Hall resistance R_{xy} and Hall resistivity ρ_{xy} can be approximated with $R_{xy} \approx \rho_{xy}/t$,

where t is the thickness of the magnetic film. For this intrinsic contribution to the EHE, materials systems with large spin-orbit-coupling and high spin-polarization will induce a large Hall signal.

Extrinsic contributions to the EHE can also have a large impact on the transverse resistance R_{xy} . These contributions can be phenomenologically divided into ‘screw’ scattering and ‘side jump’ effects, which occur when the electrons passing through the uniformly magnetized materials get deflected via anomalous scattering off impurities/defects or the surface/interfaces. The surface and interfaces are particularly important in the scattering processes of thin films,¹² and modulate the total measured Hall effect considerably. Therefore, the total EHE resistivity can be written as:

$$\rho_{xy}^M = \Phi_{ss}\rho_{xx} + \left(\kappa^{sj} - \frac{e^2}{8\pi^3\hbar} \int_{\text{BZ}} \vec{\Omega}(\vec{k}) d^3k \right) \rho_{xx}^2, \quad (2)$$

where Φ_{ss} is a constant to describe the strength of the skew scattering effect, and κ^{sj} is the side jump constant. As the coefficients of the quadratic ρ_{xx}^2 term cannot be easily separated, they are usually combined into a single constant κ .

Experimentally, the Hall resistance R_{xy} is measured as $R_{xy} = V_{xy}/I_{xx}$. The Hall resistivity ρ_{xy} can be derived after taking the geometry of the material into account. It has to be stressed that ρ_{xy}^M (and σ_{xy}^M) discussed so far are representing the values for a magnetically saturated state. The measured ρ_{xy} is a function of the magnetization M of the material and the applied magnetic field H :

$$\rho_{xy} = 4\pi R_S M + R_0 H \approx 4\pi R_S M, \quad (3)$$

where R_S is independent of the external field and is constant for a fixed temperature. The expression on the right-hand side is the approximation in the low-field limit. Note that the magnetization itself is a function of the applied field as well, which allows for the use of the EHE as an ‘analog’ electrical detector of the ferromagnetic state of the system. Indeed, the EHE has been used as a probe of the magnetization pattern, especially in diluted magnetic semiconductors, in which the ferromagnetism is usually weak. Another application of the EHE are linear magnetic field sensors in which the external field orients the magnetization resulting in a change of R_{xy} .^{13,14} However, other applications have long been ignored as the EHE is rather weak in traditional 3d transition metals.

Engineered materials systems (e.g. heterostructures and multilayers) were demonstrated to have large, enhanced EHE magnitudes,^{12,15} opening up a wide range of novel practical uses. In fact, the EHE is a promising read-out approach for memory devices as the output signal is directly corresponding to the magnetization state. If the magnetic properties show discrete and distinguishable states, these states can be effectively read out by measuring the EHE rather than using conventional magnetoresistance schemes.

III. EXTRAORDINARY HALL BALANCE

The extraordinary Hall balance is fundamentally similar to other magnetoresistive device structures, such as an MTJ or giant MR (GMR) element, in that it combines two independent ferromagnetic layers with a suitable interlayer, however, fundamentally different when it comes to the read-out strategy. For the read-out, the current is applied in-plane, as denoted by the black arrow in Fig. 1, rather than perpendicular to the plane. Note that the two FM layers are electrically in parallel as they share common side contacts (orange). The two FM layers consist of tailored layer stacks with a defined coercive field and perpendicular magnetic anisotropy, allowing for better device scaling. The magnetic heterostructure is patterned into the shape of a cross, where the current is applied along the long axis. The Hall voltage, U_H or U_{xy} , is measured across the short axis and it is proportional to the deflected electron population resulting from the magnetization state (see Fig. 1). Note that the linear contribution from the normal Hall effect has been subtracted by fitting of the high field data (up to 1 T). The net Hall voltage is the sum of the contributions of the two FM layers. Consequently, the measured Hall voltage can be positive and large, low and close to zero, or negative and large, depending on the magnetization states. The combined Hall loop in the lower part of Fig. 1 illustrates the four possible states and the corresponding Hall resistances. From this it is clear that a ultra-high Hall resistance ratio (HRR) can be reached, which is only a matter

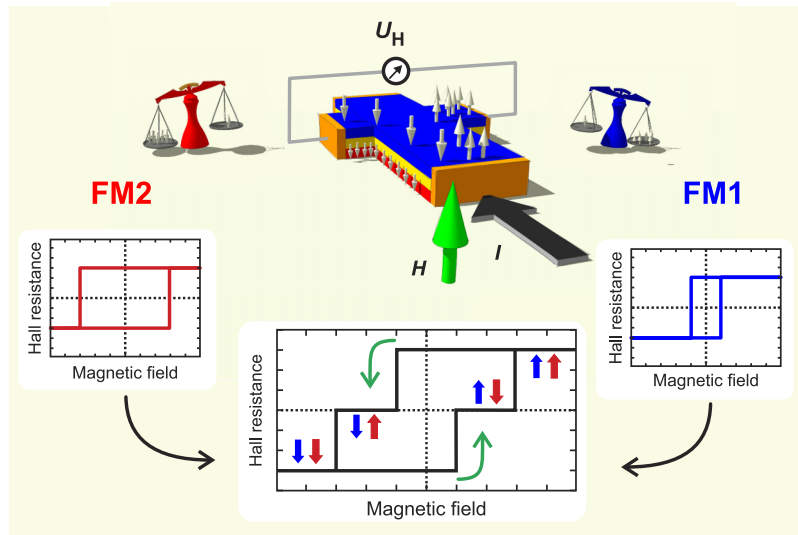


FIG. 1. Extraordinary Hall balance (EHB). The EHB, shown in the center, combines two ferromagnetic layer stacks, FM1 and FM2, separated by a thin insulating layer, into a trilayer structure, similar to an MTJ. The layers have perpendicular magnetic anisotropy. However, very different from an MTJ, side contacts are used to drive a current I through both layers, creating a parallel circuit. The layer stack is further patterned into a Hall cross in which the current is applied as shown and the Hall voltage U_H is measured perpendicular to I . A magnetic field is applied perpendicular to the layers. The Hall signals for both FM layers are shown below, whereby the layers are designed such that they have different coercive fields. When the two are coupled together in parallel, the Hall signal can either be large and negative or positive (layer magnetizations $\downarrow\downarrow$ or $\uparrow\uparrow$), or zero ($\downarrow\uparrow$ or $\uparrow\downarrow$). When, as shown in the example, the blue layer (FM1) is in the up state and the red layer (FM2) is in the down state, the two *balance* each other out, and the resulting net Hall signal is zero.

of controlling materials parameters. A magnetic field (green arrow) is applied perpendicular to the layers to allow for a manipulation of the magnetic states of the two FM layers.

As it is common for MTJs, one of the two layers can also be magnetically biased via exchange biasing from an antiferromagnetic (AFM) layer, while the other layer remains magnetically free. This allows for a shifting of the Hall loop along the magnetic field axis, essentially centering the zero Hall signal state [$\uparrow\downarrow$ or ($\downarrow\uparrow$)] around zero field. Further, depending on the thickness of the dielectric interlayer, the interlayer coupling of the ferromagnetic layers can be ferromagnetic or antiferromagnetic. A detailed discussion of the various EHB designs and options can be found in Ref. 7.

The Hall resistance ratio (HRR), defined in analogy to the TMR in MTJs, can be written as:

$$\text{HRR} [\%] = (R_H^{\uparrow\uparrow} - R_H^{\uparrow\downarrow}) / R_H^{\uparrow\uparrow} \times 100\% , \quad (4)$$

where $R_H^{\uparrow\uparrow}$ is the Hall resistance of the parallel state, and $R_H^{\uparrow\downarrow}$ is the Hall resistance of the antiparallel configuration. Making use of Eq. (3), we obtain:

$$\text{HRR} \approx 2 / \left(\frac{M_1}{M_2} - 1 \right) \quad (5)$$

where M_i are the saturation magnetization values of the i^{th} layer. As the two saturation magnetization values are getting close to one another, the HRR reaches infinity — while MTJs have a TMR ratio that only approaches infinity for half-metallic FM layers at 0 K. Effectively, engineering two magnetization values to be identical is a much more simple task from a materials perspective.

For the FM layers a number of materials combinations can be used which should contain heavy elements to get a large enough spin-orbit coupling, such as CoFeB, Co/Ni, Co/Pt and Co/Pd multilayer systems. Here, we use Co/Pt heterostructures as they offer a high EHE signal and allow for the tuning of the anisotropy via the deposition parameters. The layer structure is grown by magnetron sputtering as described in detail in Ref. 6. As an insulating interlayer, polycrystalline

or amorphous MgO or NiO was used. NiO is ideal as it can act, depending on film thickness, as an insulating barrier or an antiferromagnetic biasing layer, hence saving a target in the deposition system. For optimizing the EHB performance first the saturation Hall voltage has to be maximized, while balancing the contributions of the two Co/Pt layer stacks, and while maximizing the perpendicular anisotropy and minimizing the saturation field. A summary of the optimization process can be found in Ref. 7.

IV. MAGNETO HALL DIFFERENCE EFFECT

In the process of optimizing the EHB, the electric properties of the two FM layer stacks have to be perfectly balanced out. In principle, the EHE signal has a direct correspondence with the effective magnetization $M(H)$ in the probed piece of magnetic material, and the electric optimization should simply comprise of making the two FM layer magnetizations equal. However, in magnetic heterostructures, a large asymmetry between the Hall resistivity and the magnetic moment is found. Figure 2(a) shows the magnetic hysteresis loop (left axis) measured by magnetometry in comparison with the Hall loop (right axis) for a $[\text{Co}(0.4)/\text{Pt}(1.2)]_3$ (thickness in nm) multilayer sample with a 8-nm-thick MgO interlayer. As expected, both plots agree very well with each other. However, when enlarging the plots for small signals, as shown in Fig. 2(b), striking differences become apparent. Whereas the magnetization is almost vanishing in both the ($\uparrow\downarrow$) and ($\downarrow\uparrow$) states, the EHE response shows a residual signal. We call this discrepancy the magneto-Hall difference (MHD).

In order to better quantify this difference, we normalized both the magnetometry and Hall data to their saturation values (normalized values \hat{M} and \hat{R}). The plots of both the normalized magnetization and Hall resistance are shown in Fig. 3, as the full loops (a) and close-ups (b).

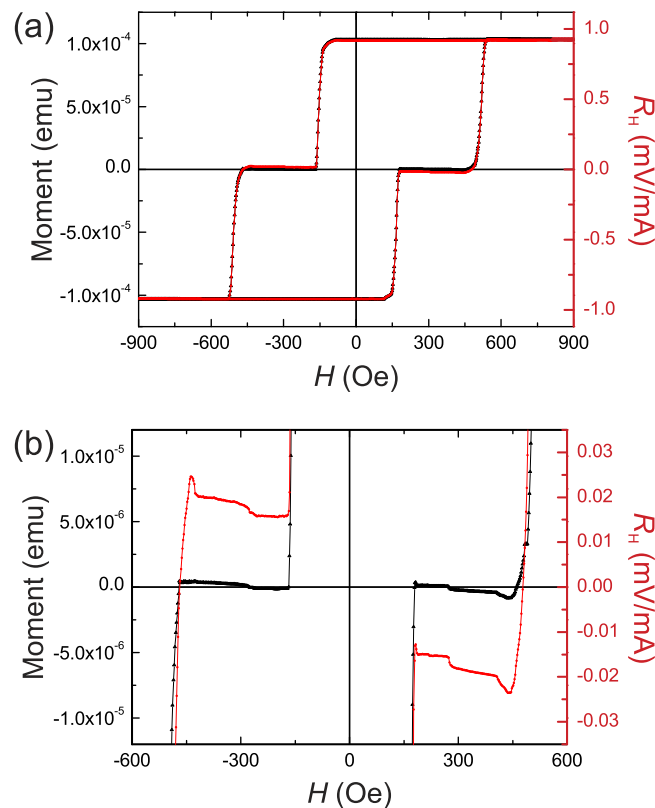


FIG. 2. Illustration of the MHD effect. (a,b) Magnetization (left axis, black) and Hall loop (right axis, red) for a $[\text{Co}(0.4 \text{ nm})/\text{Pt}(1.2 \text{ nm})]_3$ multilayer sample with an 8-nm-thick MgO interlayer between the two layer stacks. (a) shows the full loops and (b) the close-ups.

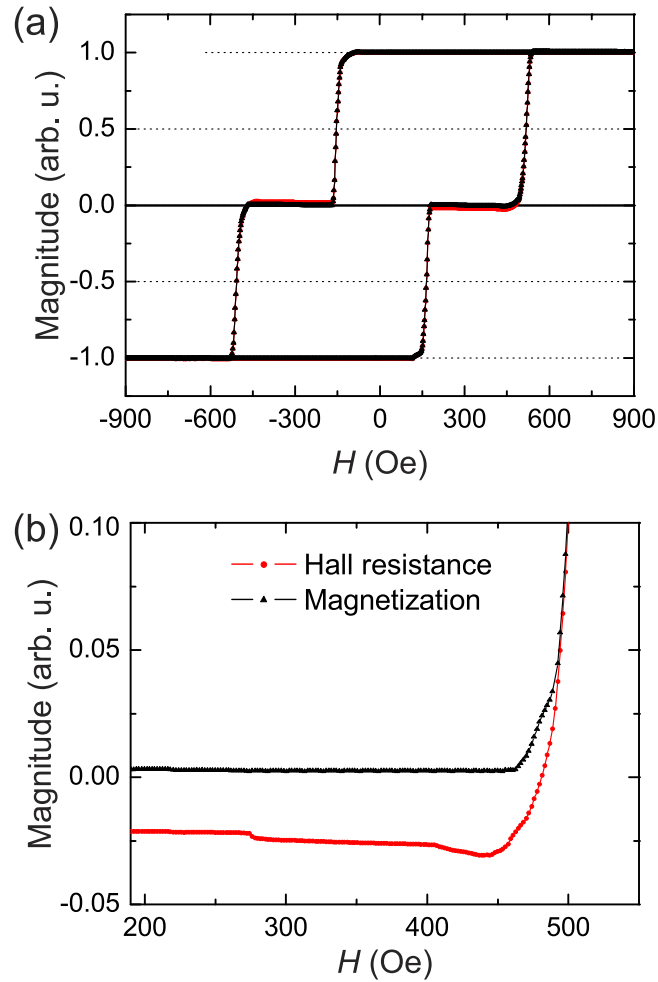


FIG. 3. Illustration of the MHD effect. (a) Normalized magnetization and Hall loop, and (b) close-up around zero signal, for positive applied fields.

Whereas the deviation of the net magnetization from zero is much less than 1%, the net Hall signal deviates by up to 5%. This deviation cannot be attributed to the formation of magnetic domains since both the magnetization and the Hall signal average over the entire sample stack. What is different from single or few layer systems is the presence of a multitude of interfaces. For example, the optimized layer stacks used here have 14 interfaces.

The intrinsic parameters in the Co/Pt multilayer system that contribute to the extraordinary Hall coefficient r_{EHE} are κ_{int} , which is directly controlled by the detailed band structure; Φ_{ss} , which arises from the impurities and defects in the crystalline structure; and the side jump constant κ_{sj} , resulting from the interfaces and surfaces. As for a magnetically balanced EHB, the κ_{in} and Φ_{ss} are identical for the two FM layers with identical thicknesses. In a previous study^{6,12} we have shown that in such multilayer structures the EHE is mainly due to side jump scattering and that it sensitively depends on the thickness of the FM layers and the spacer. It is therefore reasonable to assume that the MHD is a parameter that quantifies the side jump effect due to the interfaces.

To investigate this effect systematically, two series of samples with varying interface properties were grown and studied: $\text{NiO}(3)/[\text{Co}(0.4)/\text{Pt}(1.2)]_3/\text{MgO}(t_{\text{MgO}})/[\text{Co}(0.4)/\text{Pt}(1.2)]_3$ and $\text{NiO}(3)/[\text{Co}(0.4)/\text{Pt}(1.2)]_3/\text{NiO}(t_{\text{NiO}})/[\text{Co}(0.4)/\text{Pt}(1.2)]_3$ (thickness in nm). Further, we calculated the difference of the two field-dependent plots in the antiparallel state by

$$\text{MHD} = \hat{R}_{\uparrow\downarrow}^{\text{low}} - \hat{M}_{\uparrow\downarrow}^{\text{low}} \quad (6)$$

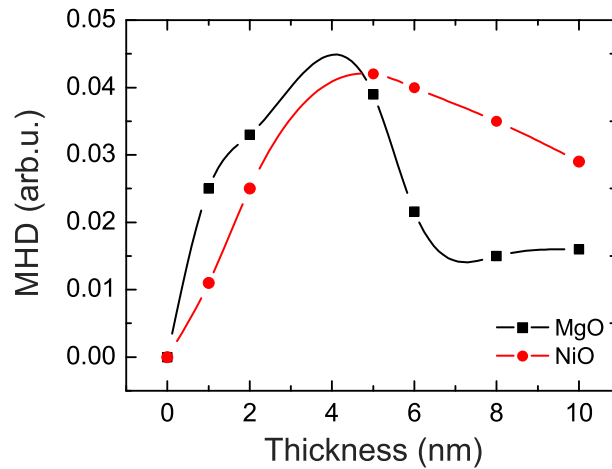


FIG. 4. Dependence of the MHD effect on the interlayer material and thickness. The MgO and NiO interlayers have thicknesses of up to 10 nm. Solid lines are guides to the eye only.

in order to quantify the effect of the interlayer material and thickness on the MHD. The resulting MHD plots are shown in Fig. 4. As can be seen, the MHD is getting smaller as the interlayer thickness increases. Also, MgO is in general a slightly preferred choice over NiO, which cannot be much thicker as it starts developing antiferromagnetic properties between 10 and 20 nm.

V. PLANAR EHB STRUCTURE

Another, radically different approach that overcomes the MHD problems stemming from the interlayer is a planar device design, shown in Fig. 5, similar to the concept presented by Segal *et al.*¹⁶ The two FM layers are identical to the ones used in the vertical EHB introduced above, but are spatially separated at the cost of a two-fold increase in device real estate. The current is applied to the circuit in parallel, and the overall Hall voltage is measured as indicated across both legs of the device in series. Consequently, the oxide/FM interfacial MHD effect can be ignored, however, all advantageous features of the standard EHB device are inherited by the planar version.

As discussed above, the Hall resistance of an individual layer is expressed by: $R_H = \rho_H/t = r_{EHE}M/t$, where R_H is the Hall resistance; ρ_H is the Hall resistivity – the intrinsic quantity that is geometry-independent; t is the thickness of the FM layer; and r_{EHE} is the EHE coefficient, characterized by the three terms introduced above, the intrinsic anomalous velocity term κ_{int} , the

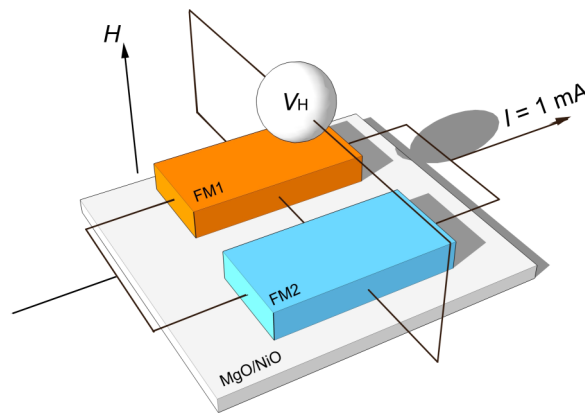


FIG. 5. Layout of the planar EHB structure. As before, both FM layers are electrically in parallel. The Hall voltage is now the sum of the individual contributions in series, instead of the parallel configuration in case of the normal (vertical) EHB.

screw scattering constant Φ_{ss} and the side jump constant κ_{sj} . The Hall resistance will induce the measured Hall voltage $V_H = R_H I$. Thus, for the planar EHB, we obtain $V_H = V_{FM1} + V_{FM2} = R_H^{FM1} I_{FM1} + R_H^{FM2} I_{FM2}$, and $I = I_{FM1} + I_{FM2}$. As the two layers are connected in parallel, we get $I_{FM1}/I_{FM2} = R_{xx}^{FM2}/R_{xx}^{FM1}$, where R_{xx} is the longitudinal resistance, characterized by the longitudinal resistivity ρ_{xx} and the thickness of the FM layer in the thin film form, $R_{xx} = \rho_{xx}/t$. Thus, the measured total Hall voltage can be written as

$$V_H = V_{FM1} + V_{FM2} \quad (7)$$

$$= I \left[R_H^{FM1} \frac{R_{xx}^{FM2}}{R_{xx}^{FM1} + R_{xx}^{FM2}} + R_H^{FM2} \frac{R_{xx}^{FM1}}{R_{xx}^{FM1} + R_{xx}^{FM2}} \right].$$

At this stage, only the low Hall resistance state is of interest. For the low Hall state, only the saturation Hall resistance has to be considered $R_H^{sat} = r_{EHE} M_S / t$, where M_S is the saturation magnetization. Consequently, the low Hall state takes the form

$$R_H^{low} = \left[r_{EHE}^{FM1} \frac{M_S^{FM1}}{t_1} \frac{\rho_{xx}^{FM2} t_1}{\rho_{xx}^{FM1} t_2 + \rho_{xx}^{FM2} t_1} - r_{EHE}^{FM2} \frac{M_S^{FM2}}{t_2} \frac{\rho_{xx}^{FM1} t_2}{\rho_{xx}^{FM1} t_2 + \rho_{xx}^{FM2} t_1} \right]. \quad (8)$$

Note that if the stoichiometry of Co and Pt in the [Co/Pt]₃ layer is kept the same as before, the longitudinal resistivity ρ_{xx} does not change with the thickness; and M_S is proportional to the thickness of the layer, i.e., $M_S = a \cdot t$, where a is a constant. Therefore,

$$R_H^{low} = a \left[r_{EHE}^{FM1} \frac{t_1}{t_1 + t_2} - r_{EHE}^{FM2} \frac{t_2}{t_1 + t_2} \right]. \quad (9)$$

For a planar EHB, as FM1 and FM2 share the same interface, all three contributions to the total EHE should be identical, thus $r_{EHE}^{FM1} = r_{EHE}^{FM2}$. Therefore, to balance out the planar EHB, the main requirement is to synthesize two FM layers with the same thickness, and to control the nanolithography well enough to achieve the same coercivity for the switching of the two structures.

VI. SUMMARY AND CONCLUSIONS

In summary, we have shown that interfacial effects, at the interface between the FM layer stacks and the insulating barrier, are responsible for the difference between the normalized magnetization and Hall voltage in the compensated state of an EHB device element. The MHD effect can be used to our advantage as it provides an extra dimension of parameter space in which to tune the properties of the EHB. In fact, by taking advantage of the interfacial effect, different types of the EHB for various purposes can be realized.⁷ By optimizing the EHB device fully considering the MHD effect, and the HRR can be pushed up to ~47,000%.⁷ Moreover, since the MHD is solely an interface effect, the concept of the planar EHB was introduced. Here, by simply assuring identical thicknesses of the FM layer stacks, ultra-low compensated Hall responses will be possible, opening the door to a large variety of logic, memory, and sensor applications in the future.

ACKNOWLEDGMENTS

S. L. Z. and T. H. acknowledge financial support by the Semiconductor Research Corporation (SRC).

¹ S. Basu, D. Pavlidis, T. Theis, K. Bergman, and J. Candelaria, "Report to the National Science Foundation on The Workshop for Energy Efficient Computing," April 14-15 (2015).

² W. J. Gallagher and S. S. P. Parkin, "Development of the magnetic tunnel junction MRAM at IBM: From first junctions to a 16-Mb MRAM demonstrator chip," *IBM J. Res. Dev.* **50**, 5–24 (2006).

³ A. Ney, C. Pampuch, R. Koch, and K. H. Ploog, "Programmable computing with a single magnetoresistive element," *Nature* **425–487**, 485 (2003).

⁴ I. Sinova and J. Žutić, "New moves of the spintronics tango," *Nature Mater.* **11**, 368–371 (2012).

⁵ S. Ikeda, J. Hayakawa, Y. Ashizawa, Y. M. Lee, K. Miura, H. Hasegawa, M. Tsunoda, F. Matsukura, and H. Ohno, "Tunnel magnetoresistance of 604% at 300 K by suppression of Ta diffusion in CoFeB/MgO/CoFeB pseudo-spin-valves annealed at high temperature," *Appl. Phys. Lett.* **93**, 082508 (2008).

- ⁶ S. L. Zhang, Y. Liu, L. J. Collins-McIntyre, T. Hesjedal, J. Y. Zhang, S. G. Wang, and G. H. Yu, "Extraordinary Hall balance," *Sci. Rep.* **3**, 2087 (2013).
- ⁷ S. L. Zhang, A. A. Baker, J.-Y. Zhang, G. H. Yu, S. G. Wang, and T. Hesjedal, "Universal Magnetic Hall Circuit Based on Paired Spin Heterostructures," *Adv. Electron. Mater.* **1**, 1400054 (2015).
- ⁸ S. L. Zhang, L. J. Collins-McIntyre, J.-Y. Zhang, S. G. Wang, G. H. Yu, and T. Hesjedal, "Nonvolatile full adder based on a single multivalued Hall junction," *SPIN* **3**, 1350008 (2013).
- ⁹ S. L. Zhang, J.-Y. Zhang, A. A. Baker, S. G. Wang, G. H. Yu, and T. Hesjedal, "Three dimensional magnetic abacus memory," *Sci. Rep.* **4**, 6109 (2014).
- ¹⁰ R. Karplus and J. M. Luttinger, "Hall effect in ferromagnetics," *Phys. Rev.* **95**, 1154 (1954).
- ¹¹ N. Nagaosa, J. Sinova, S. Onoda, A. H. MacDonald, and N. P. Ong, "Anomalous Hall effect," *Rev. Mod. Phys.* **82**, 1539 (2010).
- ¹² S. L. Zhang, J. Teng, J. Y. Zhang, Y. Liu, J. W. Li, G. H. Yu, and S. G. Wang, "Large enhancement of the anomalous Hall effect in Co/Pt multilayers sandwiched by MgO layers," *Appl. Phys. Lett.* **97**, 222504 (2010).
- ¹³ J. Moritz, B. Rodmacq, S. Auffret, and B. Dieny, "Extraordinary Hall effect in thin magnetic films and its potential for sensors, memories and magnetic logic applications," *J. Phys. D: Appl. Phys.* **41**, 135001 (2008).
- ¹⁴ A. Gerber and O. Riss, "Perspective of Spintronics Applications Based on the Extraordinary Hall Effect," *J. Nanoelectron. Optoe.* **3**, 35 (2008).
- ¹⁵ C. L. Canedy, X. W. Li, and Gang Xiao, "Large magnetic moment enhancement and extraordinary Hall effect in Co/Pt superlattices," *Phys. Rev. B* **62**, 508–519 (2000).
- ¹⁶ A. Segal, M. Karpovski, and A. Gerber, "Sixteen-state magnetic memory based on the extraordinary Hall effect," *J. Magn. Magn. Mater.* **324**, 1557–1560 (2012).